Mode transition and nonlinear self-oscillations in the beam-driven collisional discharge plasma

Hae June Lee and Jae Koo Lee
Pohang University of Science and Technology, Pohang 790-784, South Korea

(Received 13 February 1998; accepted 19 May 1998)

Nonlinear dynamics and self-oscillations in a dc beam-driven collisional discharge are investigated with particle-in-cell simulation and theoretical estimation. Three different modes, anode-glow, temperature-limited, and double-layer modes, are observed in the system. A theory for the critical voltage of mode transition between temperature-limited and anode-glow modes is in good agreement with the simulation results. The mechanism of low frequency self-oscillation in the double layer mode is examined along with period-doubling and chaotic oscillations. © *1998 American Institute of Physics.* [S1070-664X(98)03108-5]

I. INTRODUCTION

The investigation of self-oscillation and chaos in a beam-injected plasma system by experiments[1–7] and simulation[8] has received much attention during the past ten years. The experiments are performed in a plasma device consisting of an electron-emitting cathode with filaments surrounded and a current-collecting anode. The injected electron beam generates plasma by ionizing neutral gas, and interacts with the plasma.

In the low pressure regime of this system, there is hysteresis in the discharge current vs the applied dc voltage characteristic $I(V_d)$, and a sudden mode transition between two stable modes.[5,6,8] The lower branch of the $I(V_d)$ curve is called the anode-glow mode (AGM) and the upper branch the temperature-limited mode (TLM). In the AGM, the space-charge effect ruled by the Child–Langmuir law is dominant, and the ionization process occurs only in the regime near the anode which is called the anode-glow regime. The discharge current in this mode is much smaller than the injected beam current, since the majority of the injected electrons is reflected by the virtual cathode. In the TLM, the ionization process occurs in the entire system except for the sheath regions near the anode and the cathode, and the density of the ionized plasma is much higher than that of the beam. The discharge current in the TLM is almost the same as the beam current.

For a sufficiently high gas pressure, the double-layer mode (DLM) appears. In this mode, the elastic collision between the neutral and the injected beam is dominant, which induces the spread of the beam velocity. Hence the system does not have a cold beam interacting with plasma any more. Ion deceleration due to collision with neutral gas makes an ion-rich region, which leads to a potential drop within a short range, which forming a double layer (DL). This mode is shown in the right-hand side of the V_d vs pd mode-transition curve similar to the Paschen curve. DL formation was intensively studied,[9–14] and the oscillations in the DL was reported,[15,16] most of which are for the collisionless system.[10–15] It is noted that DL formation is due to the ion deceleration by the collision with neutrals in the high pressure regime. We have observed the self-oscillations in this mode, whose frequencies are lower than the ion plasma-frequency.

These three modes are determined by the discharge parameters such as the gas pressure p, the applied dc voltage V_d, the current density J_b of the injected beam, and the system length d. Under particular conditions, these modes show self-oscillations and various routes to chaos such as period-doubling,[1,3,5,6,8] intermittency,[2] and quasiperiodicity[4] by varying some discharge parameters without an external driver[3–5] or with an external modulation.[1,2,6,8] These chaotic oscillations occur especially around the points of mode transition in the hysteresis curve.[3,4] The oscillation mechanism in the AGM is related to a potential-relaxation oscillation due to double-layer formation by ion trapping.[8] However, the oscillation mechanism in the TLM is very different from that in the AGM, and still unknown.[5] The oscillation mechanism in the DLM is similar to that of the AGM, but different in that there is no virtual cathode which traps ions and in that the ion depletion is not related to the Pierce–Buneman instability which is caused by a fast-moving electron beam.

In this study, our primary focus is on the mechanisms of the mode transition from the AGM to the TLM and self-oscillations. It is revealed that the mode-transition mechanism is related not to the electron but to the ion motion. We propose a theory for this phenomenon and compare with the simulation results in Sec. II.

In the DLM, there are low frequency oscillations which are driven to chaos through period-doubling as voltage is increased. The oscillation mechanism of this mode is discussed and compared with experimental result in Sec. III. Finally, a summary and discussions are presented in Sec. IV.

II. THREE MODES

A. Model for simulation

We consider the simplest thermionic system, one-dimensional planar diode, simulated with the one-dimensional particle-in-cell code, XPDP1.[17] The code is modified so that we can deal with the beam and the plasma

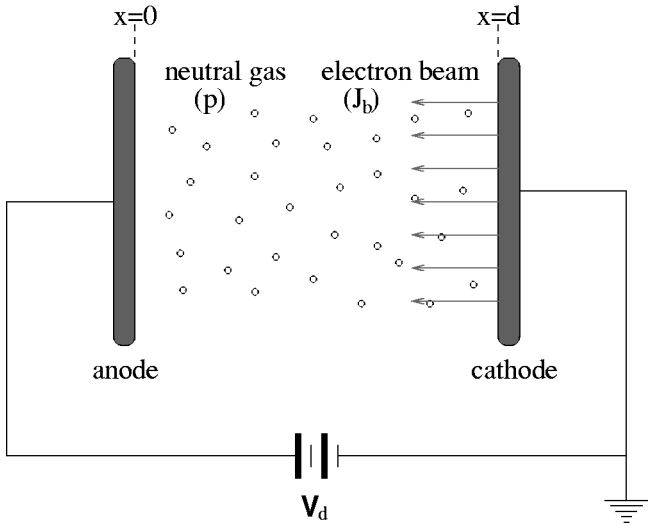

FIG. 1. Schematics of the beam-driven discharge-plasma system. The input variables are the system length d, the neutral gas pressure p, the current density of the injected beam J_b, and the applied voltage V_d.

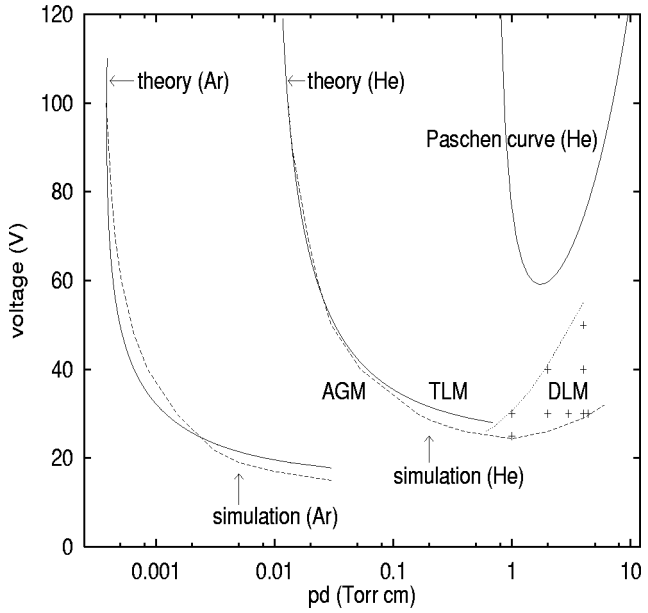

FIG. 2. The pd vs V_d phase diagrams for three modes, AGM, TLM, and DLM. The transition boundaries of the AGM and the TLM by Eq. (13) are compared with simulations for argon and helium gases. The Paschen's breakdown curve for helium gas with secondary emission coefficient $\gamma = 0.3$ is shown as solid curves.

separately. In order to investigate the trajectory of the beam, especially in the TLM, we treat the beam as a separate species from the bulk electrons. The Monte-Carlo collision subroutine of the XPDP1 code has been changed so that the beam particles are converted to bulk electrons when they lose energy by collisions. The positively-biased anode with dc voltage V_d is located at the position $x=0$ and the grounded cathode is separated by a gap distance d, and an electron beam with a current density J_b is injected into the diode from thermionic filaments on the cathode, as shown in Fig. 1. The pressure of the uniform background neutral gas is p. The electron velocity distribution function (EVDF) $f_b(x,v)$ of the injected beam is half Maxwellian on the cathode with a filament temperature T:[18]

$$f_b(d,v) = \frac{n_b}{\sqrt{\pi} v_{\mathrm{th}}} \exp\left(- \frac{v^2}{v_{\mathrm{th}}^2} \right), \tag{1}$$

where n_b is the number density of the beam particles and $v_{\mathrm{th}} \equiv (2kT/m_e)^{1/2}$ is the thermal velocity of the injected beam with temperature T. k and m_e are the Boltzmann constant and the electron mass, respectively. The control parameters of this system are p, d, V_d, J_b, and T. The boundary conditions of the simulation in addition to Eq. (1) are

$$\phi(0,t) = V_d, \quad \phi(d,t) = 0, \tag{2}$$

where $\phi(x,t)$ is the electrostatic potential. The initial condition of the simulation are

$$n_i(x,0) = 0, \ \ n_e(x,0) = 0, \tag{3}$$

where $n_i(x,t)$ and $n_e(x,t)$ are the number densities of ions and electrons created by ionization, respectively. The simulation parameters are $J_b = 1$ A/m^2, grid size $\Delta x = 0.5 \sim 1 \lambda_D$ (Debye length), time step $\Delta t = 0.2 \sim 1$ ns, and the area of each electrode is 0.01 m^2. We simulate with two species of neutral gas, helium and argon. The simulation results shown in Figs. 3–8 below are for helium gas, but the results are almost the same for argon gas.

We consider only an unmagnetized system with a dc applied voltage and constant beam current without external modulations. A magnetized, pulsed-beam injected, or ac voltage-driven system is the subject for a future study.

B. Anode-glow, temperature-limited, and double-layer modes

By varying the input parameters, we have found that there are three distinctive steady-state modes besides the extinguished mode; in the latter, the ionization process seldom happens. The regimes of the modes are specified in a V_d vs pd diagram, as shown in Fig. 2, similar to the Paschen's breakdown curve without a beam component. The first one is the anode-glow mode which appears in a low voltage or a low pressure regime. The second one is the temperature-limited mode which appears in a high voltage and an intermediate pressure regime. The third one is the double-layer mode which appears in a high pressure and an intermediate voltage regime. Some experiments reported the existence of double layers in the beam-induced plasma system, but the regime of this mode in a collisional system was not extensively studied in the past.

Figure 3 shows various properties of these modes. In the AGM, the ionization occurs only in the vicinity of the anode, where electrons accelerated by the applied voltage have enough energy to ionize the neutrals. The created ions move toward the cathode, some of which are trapped in the potential well by energy loss from collision with neutrals. The total charge density is an electron-rich state, and the resulting potential is a well-type as shown in Fig. 3(a). The discharge current of this mode is smaller than the incident beam current, because a substantial fraction of the injected beam is reflected by the virtual cathode. Sometimes this mode exhib-

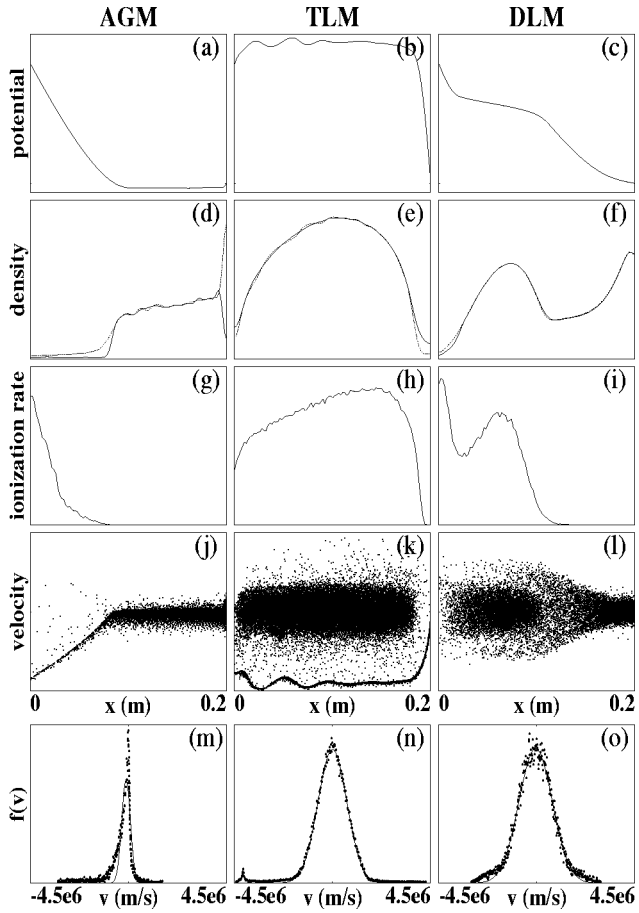

FIG. 3. (a)–(c) Potential profiles (scale: $-3-50$ V); (d)–(f) electron (dotted lines) and ion (solid lines) density profiles (scales: $0-1.5\times10^{13}$, $0-3\times10^{14}$, and $0-7.5\times10^{13}$ m^{-3} for each mode, respectively); (g)–(i) ionization rate profiles (scales: $0-10^{17}$, $0-6\times10^{18}$, and $0-6\times10^{17}$ s^{-1} for each mode, respectively); (j)–(l) velocity vs position phase spaces (scale: $-4.5\times10^{6}-4.5\times10^{6}$ m/s); and (m)–(o) velocity distribution-functions for the steady-state AGM, TLM, and DLM. $p=2.3$ mTorr, 10 mTorr, and 200 mTorr for the cases of each mode, respectively, with the same $V_d=40$ V and $d=20$ cm.

its self-oscillation whose mechanism is examined by Greiner *et al.*;[8] a repetition of the ion trapping by charge exchange, double-layer formation, and ion depletion by the Pierce–Buneman instability. The velocity distribution of this mode is far from Maxwellian as shown in Fig. 3(m).

In the TLM, the ionization occurs in the entire plasma regime, and the resulting density is much higher than that of the AGM. The discharge current is the same as the injected beam current since the electron beam is accelerated to the anode by the plasma potential through the cathode sheath. The velocity distribution in Fig. 3(n) shows a bump on the tail of a Maxwellian distribution, which induces a beam–plasma instability.[19,20] In some cases, this instability grows to a large amplitude, finally driving period-doubling or chaotic oscillations. Even though the critical voltage of mode transition is determined by the product of the gas pressure and the system length, the oscillations are affected by individual parameters, especially by the system length. Recently, a common parameter defined as the ratio of interaction length to the synchrotron slippage length has been proposed for a simplifying the measure of self-oscillation and chaos in several beam–plasma interaction systems.[21–23] The regimes where various oscillations such as limit-cycle (1P), period-doubled (2P), period-quadrupled (4P), quasiperiodic (QP), and chaotic (C) oscillations appear are indicated by this parameter, almost independently of other input parameters. As this parameter increases, the system becomes chaotic. Since the interaction length is related to the system length in the TLM, the larger system length shows the more chaotic oscillations. It is verified in our simulation results. The common parameter is also shown to be a good measure of chaos for the infinite homogeneous beam–plasma instability.[24]

In the DLM, elastic collisions are so frequent that the injected beam slows down with velocity distribution broadened, losing the cold beam characteristics. It shows a monotonic potential drop ($\Delta\phi>kT_e/e$) around the center of the system, which causes a distinctive feature of a double layer. This is achieved by a dipole-like charge distribution with an ion hole in the center region. The ionization profile is similar to that of the AGM except that there is a bump at the high potential side of the DL due to the large electric field between the high and low potential sides. Bohm and Torvén reported that an ion-density cavity can support large potential drops by theory and simulation.[14] While they started from an artificial initial condition of the ion-density distribution, our results are self-consistently established by the ion–neutral collision, and the resultant potential drop is similar. Various types of DL's were reported;[10] the strong double layer with $v_d>v_{\rm th}$,[11] the ion-acoustic double layer,[12] and the slow ion-acoustic double layer[13] with $v_d<v_{\rm th}$, where v_d and $v_{\rm th}$ are the drift velocity and thermal velocity of the electron. DL shown in this study is a slow ion-acoustic double layer, whose potential difference $\Delta\phi<5kT_e/e$, and $v_d\simeq0.1v_{\rm th}$ (almost current-free). The electron temperature T_e is about 2–3 eV, which is larger than the ion temperature T_i which is less than 0.1 eV. The mechanism of the formation of an ion-acoustic-type DL is explained by an anomalous resistivity in front of the potential drop.[12] In this system, it is mainly due to the ion deceleration by charge-exchange collision. When we turn off the ion collisional process in the simulation, there is no DL formation in the same parameter regime. But for a higher voltage or higher neutral gas pressure, DL can be built up without ion collision. Low frequency oscillations are observed in the low voltage regime of the DLM, which can be driven to chaos through a period-doubling route. Most experiments reporting the self-oscillation and chaos are performed in a low voltage regime[1–4,6] except for that by Capeau *et al.*,[5] whose oscillation frequency is on the order of kHz. The parameter regime of the experiment by Qin *et al.*[3] is $V_d=7-10$ V and $pd=0.1-0.4$ (Torr cm) with Ar, where a period-doubling route to chaos is observed as V_d is increased. Considering the low voltage less than the ionization energy of argon gas (15.76 eV), the beam current and energy should be sufficiently large. It is considered as the DLM regime. The parameter regime of experiment by Klinger *et al.*[6] is $V_d=16-25$ V and $pd=0.001-0.05$ (Torr cm) with Ar, which is the AGM regime. Considering this, we deduce that the experimentally observed low frequency oscillations are in the regime of the AGM and the DLM.

C. AGM→TLM mode transition

As reported in many experiments,[2–6] there is sudden mode transition and hysteresis in the current-voltage characteristic $I(V_d)$ curve between the AGM and the TLM. In this section, we establish a theory for the mode transition and compare with our simulation results. In the initial state, if the applied voltage difference is sufficiently larger than the temperature of emitted electrons from the cathode ($V_d \gg kT/e$), the fluid theory known as the Child law gives the relation between V_d and the current flowing through the diode,

$$J_c = \frac{4}{9}\epsilon_0 \left(\frac{2e}{m_e}\right)^{1/2} \frac{V_d^{3/2}}{d^2}, \tag{4}$$

where J_c is the largest stable current density of the diode, and ϵ_0 and e are the permittivity of free space and unit charge. For the injected current density J_b less than J_c, the corresponding potential profile is

$$\phi(x) = V_d(1 - x/d)^{4/3}, \tag{5}$$

and there is no virtual cathode. In the opposite case, $J_b > J_c$, the virtual cathode is formed near the cathode, and some portions of the injected beam particles are reflected by the virtual cathode. In this case, the potential profile should be obtained by solving the steady-state Vlasov equation. Langmuir's solution[25] for this problem is

$$\pm \xi(\eta) = \frac{1}{\sqrt{2}} \int_0^{\eta} \frac{d\tilde{\eta}}{\sqrt{e^{\tilde{\eta}} - 1 \pm e^{\tilde{\eta}} \mathrm{erf}(\sqrt{\tilde{\eta}}) \mp 2\sqrt{\tilde{\eta}/\pi}}}, \tag{6}$$

where η and ξ are the normalized potential and length, respectively, as

$$\eta = \frac{e(\phi - \phi_{\min})}{kT}, \tag{7}$$

$$\xi = (x - x_{\min})\lambda_D \sqrt{\frac{1}{2}\exp\left(\frac{e\phi_{\min}}{\frac{1}{2}m_e v_{\mathrm{th}}^2}\right)}, \tag{8}$$

where $x_{\min}$ and $\phi_{\min}$ are the the position of the minimum potential and the potential at the position, respectively; λ_D is the Debye length of the electron beam.

If we consider a small current density (but even larger than J_c) case, the potential difference between the cathode and the virtual cathode is much smaller than the applied voltage V_d,

$$\frac{|\phi_{\min}|}{V_d} \ll 1. \tag{9}$$

The temperature of the emitted electrons is assumed to be much smaller than the ionization energy ($\varepsilon_{iz} > kT/e$). For this low current density and low energy beam, we estimate the boundary between the AGM and the TLM. The boundary is determined as follows: at the first stage [Fig. 4(a)], the ionization process happens only in the anode-glow regime (AGR) where the energy of the accelerated beam is greater than the ionization energy. With simple estimation, we calculate the length of AGR (l),

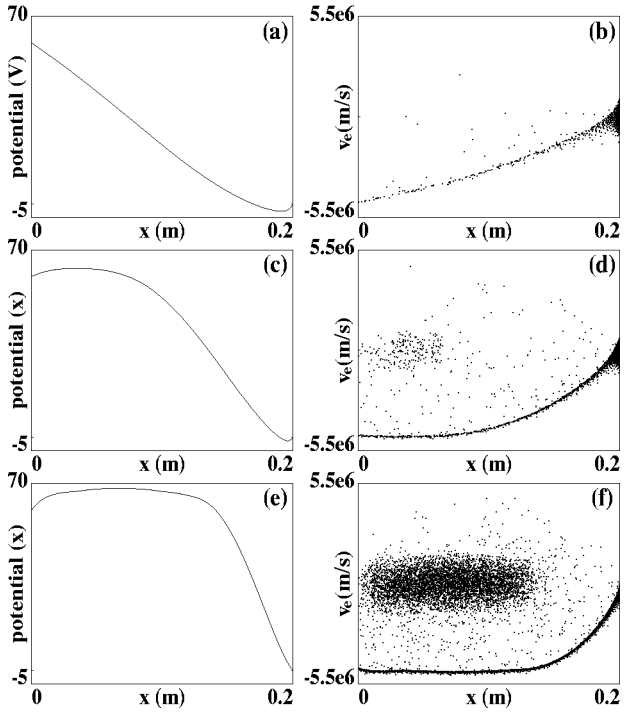

FIG. 4. Mode-transition process from the AGM to the TLM. Potential profiles and velocity vs position phase spaces at (a),(b) $t=3$ μs; (c),(d) $t=15$ μs, and (e),(f) $t=29$ μs for $d=20$ cm, $p=2$ mTorr, and $V_d=60$ V.

$$l \simeq d\left(\frac{V_d - \varepsilon_{iz}}{V_d}\right). \tag{10}$$

If the number of the ions created by ionization in the AGR is smaller than that of ions flowing to the cathode out of AGR, the AGM state is sustained. If the ion creation exceeds the ion loss in the AGR, the charge density in the AGR increases positively and the potential increases, because of the slow motion of the heavy ion. With the increased potential, more electrons which ionize neutrals are trapped in the AGR [Fig. 4(b)]. Thus the AGR is extended close to the cathode, and finally the system is driven to a TLM [Fig. 4(c)]. The condition for the TLM is

$$n_g \langle \sigma_{iz} v_e \rangle > \langle v_i \rangle / l, \tag{11}$$

where $\langle v_i \rangle = (2e\bar{\phi}/m_i)^{1/2}$ is the mean ion velocity in the AGR, $\langle \sigma_{iz} v_e \rangle = \sigma_{iz}(\bar{\phi})(2e\bar{\phi}/m_e)^{1/2}$ is the ionization rate, and $\bar{\phi}$ is the average potential of the AGR, respectively. The ionization cross section for He is given by[26]

$$\sigma_{iz}(\varepsilon) = \begin{cases} 0, & 0 \leqslant \varepsilon < \varepsilon_{iz}, \\ 10^{-17}(\varepsilon - \varepsilon_{iz})/[(\varepsilon + 50)(\varepsilon + 300)^{1.2}], & \varepsilon \geqslant \varepsilon_{iz}. \end{cases} \tag{12}$$

With these relations, we obtain the AGM–TLM boundary as a function of pd, similar to the Paschen's breakdown curve:

$$V_d > \frac{\sqrt{\frac{m_i}{m_e}}\varepsilon_{iz}\sigma_{iz} n_g d}{\sqrt{\frac{m_i}{m_e}}\sigma_{iz} n_g d - 1}, \tag{13}$$

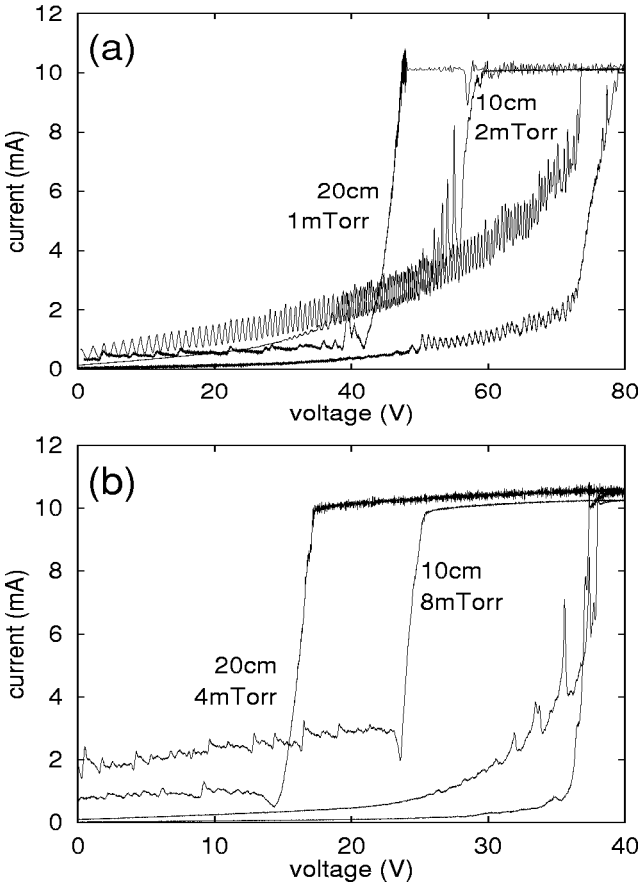

FIG. 5. Hysteresis curves for the same pd but different p and d values. (a) $pd=0.02$ (Torr cm) and (b) $pd=0.08$ (Torr cm).

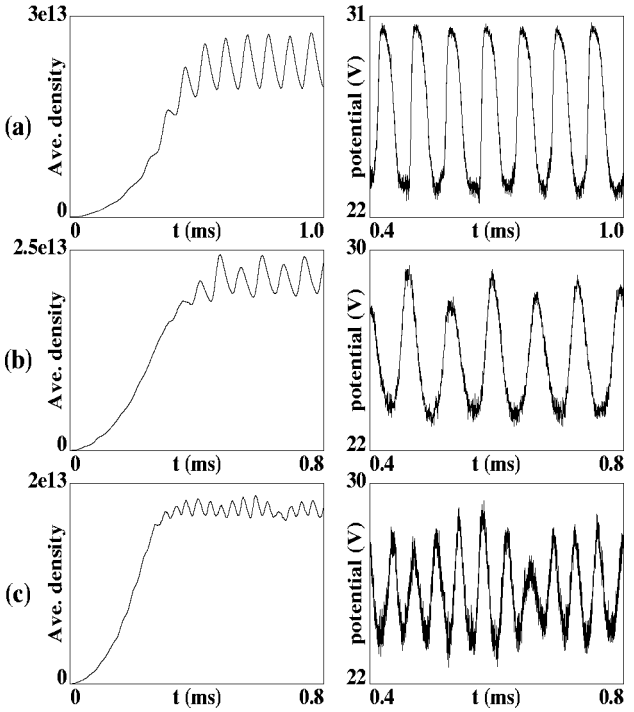

FIG. 6. Time evolutions of the average ion densities and the potentials at $x=5$ cm for the DLM, $p=0.2$ Torr and $d=20$ cm case. (a) Self-oscillation with $V_d=30$ V, (b) period-doubled oscillation with $V_d=32.5$ V, and (c) chaotic oscillation with $V_d=33.5$ V.

where $n_g=3.25\times10^{22}p$ (Torr) m^{-3} for room temperature (297 K).

This equation does not include the effect of the beam current, since we have neglected the effect of the virtual cathode. However, if the injected current increases, the potential difference due to the virtual cathode affects the size of the AGR, and the boundary moves down to a lower voltage regime. The effect of a large cathode temperature plays a similar role to that of a large current density, which moves the boundary down to the lower voltage regime. In Fig. 2, the boundary lines from Eq. (13) compare well with our simulation results for two gas species, helium and argon, which have different ion masses. The mass ratio of an ion to an electron plays an important role in the transition as shown in Eq. (13). The simulated current density of the beam is $J_b=1\mathrm{A/m}^2$ with cathode temperature $kT=1$ eV$<\varepsilon_{iz}$, which satisfies the condition of Eq. (9), where $\varepsilon_{iz}=24.5$ and 15.76 eV for He and Ar, respectively. The typical temperature of hot filament is near or above 0.2 eV, and it plays a minor role if it is much smaller than the sheath potential and ionization energy and not so much smaller than the virtual cathode potential. We have varied p and d values with the same pd product. Simulated hysteresis curves are plotted in Fig. 5, which are obtained by increasing the applied voltage slowly and decreasing it after the mode transition. The rising time is 1 ms, which is much larger than the mode-transition time-scale. The mode transition happens at $V_d=72$ V for the $pd=0.02$ (Torr cm) case, and at $V_d=37$ V for the $pd=0.08$ (Torr cm) case. The mode-transition voltage is affected only by the product of p and d, but the areas of the hysteresis curves are different for different d values. This means that even though the mode transition is determined by the value of pd, the dynamics of the system is strongly related with each value of p and d. The low frequency oscillations in the AGM before and after the mode transition are also shown.

III. OSCILLATIONS IN THE DOUBLE-LAYER MODE

In the double-layer regime, self-oscillations are observed just above the transition boundary between the AGM and the DLM as shown in Fig. 6(a). The oscillation frequency is very low, approximately tens of kHz, which is much smaller than the ion plasma frequency of approximately an order of MHz. Since the elastic collision is dominant and the injected beam spreads out by the collision, there exists no longer beam–plasma or Pierce–Buneman instability. Thus the oscillation mechanism of this mode is different from those of the AGM and the TLM. As the external voltage increases, this oscillation becomes a period-doubled oscillation [Fig. 6(b)], and finally a chaotic oscillation [Fig. 6(c)]. The fluctuation amplitude decreases as the external voltage increases, finally generating a steady-state DL.

It was reported that the propagating DL in collisionless finite-length plasmas shows a low-frequency oscillation (2.5 kHz).[15] There are two stages of the oscillation; the first one is a strong propagating DL which is accompanied by a broad negative potential at its low potential side, and the second

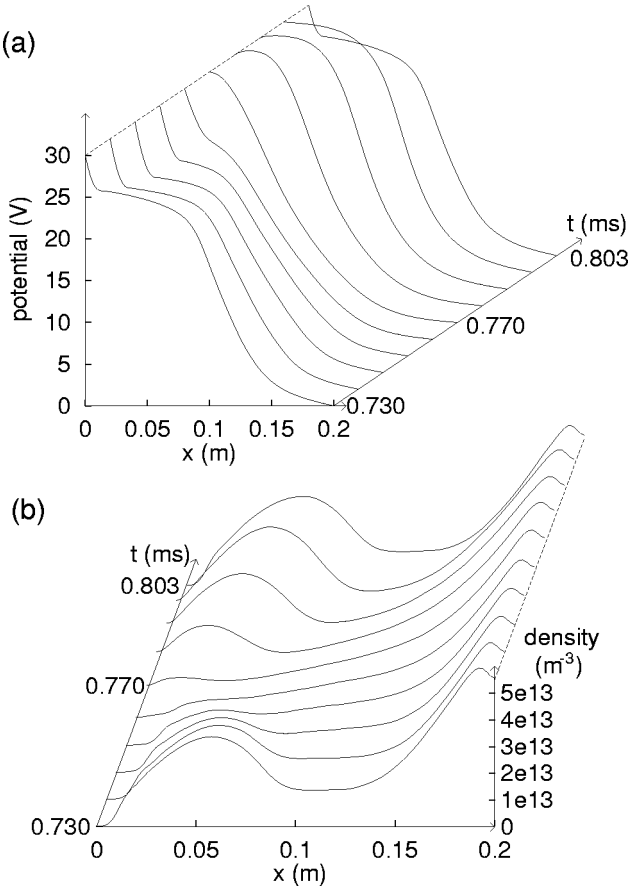

FIG. 7. Time evolutions of (a) the potential profiles and (b) the ion-density profiles for the $p=0.2$ Torr, $d=20$ cm, and $V_d=30$ V case.

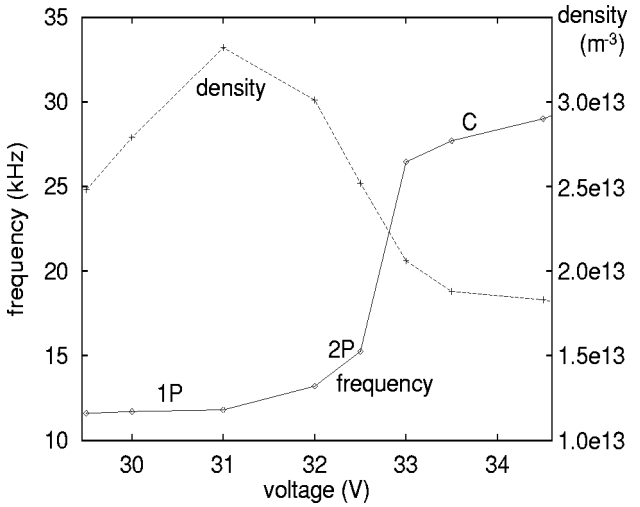

FIG. 8. Average ion density and fundamental frequency vs applied voltage for the $p=0.2$ Torr, $d=20$ cm case. The regimes where self-oscillation, period-doubled, and chaotic oscillations appear are marked 1P, 2P, and C, respectively.

one by a fast increase of the potential in the entire plasma shortly after the DL reaches the anode. This is a potential-relaxation oscillation,[10] which is also shown in the plasma diode with injected electron and ion beams with equal temperatures.[18] The propagation velocity is associated with the ion transit-time of the DL. The oscillation mechanism in the collisional discharge plasma is similar to this, except that there is no negative potential at its low potential side, and that the DL formation and oscillation are related to the collision effect.

The time evolutions of oscillating DL are shown in Fig. 7. If the potential difference of the DL is larger than the ionization energy ε_{iz}, the densities of electrons and ions increase at the high potential side. When the densities increase sufficiently, the breaking of charge neutrality due to fast electron loss induces large electric field which drives the ions to the low potential side (from $t=0.73$ to $t=0.77$ ms). After the ion loss of the high potential side, the increased potential difference causes fast ionization, and the densities increase again (from $t=0.77$ to $t=0.803$ ms). Repetition of these processes is the mechanism of self-oscillation in the collisional DLM, which is the same with that of the reported experiment.[16] Experimentally, low frequency fluctuation of the ionization front in the TLM→AGM transition regime was observed.[7]. The fluctuating ionization front produces ion bunches that propagate in the direction of the electric field, which agrees very well with our simulation results shown in Fig. 7(b). The propagation speed of the ion bunches in Fig. 7(b) is about 1.6×10^3 m/s, which is ion thermal velocity rather than ion-acoustic wave velocity.

For a large applied voltage ($V_d\gtrsim35$ V), when the ion loss due to the large electric field exceeds the ion creation due to ionization, the oscillation disappears. The DL, however, is still maintained because of the decelerated ions by a charge-exchange collision. For a larger applied voltage, the ions accelerated by the large electric field move to the cathode, and the mode transits to the TLM.

Figure 8 shows the dependencies of the dominant oscillation frequency and the average density to the applied voltages for the $p=0.2$ Torr and $d=20$ cm case. The oscillation frequency suddenly increases where $V_d>32$ V, and saturates again where $V_d>33$ V. Between these two values at 32.5 V, a period-doubled (2P) oscillation appears. It is very similar to the experimental results,[16] where a period-doubling route to chaos of the DL oscillations in the collisional discharge plasma was reported. The density decreases as the voltage increases, since ion loss exceeds ion creation. For a larger voltage, the density increases again, especially in the TLM. The plasma density is mainly affected by the neutral gas pressure, while the oscillation types—1P, 2P, or chaotic oscillations—are mainly affected by the applied voltage. For a fixed voltage case ($V_d=30$ V), the average density is 8.7×10^{13} m^{-3} for $p=0.15$ Torr which linearly decreases to 2.4×10^{13} m^{-3} for $p=0.22$ Torr, and the oscillation frequency is 4.74 kHz for $p=0.15$ Torr which linearly increases to 13.4 kHz for $p=0.22$ Torr. All of these are 1P oscillations with the same voltage.

IV. SUMMARY AND DISCUSSION

The mode transition and the nonlinear oscillations in the dc-driven beam-injected collisional discharge plasma are studied using a particle-in-cell simulation. For various products of pressure and system length (pd) and dc voltage (V_d) values, three different modes are observed. The mechanism

of mode transition between the AGM and the TLM is elucidated. The estimated boundaries of those two modes agree well with the simulation results. In addition to the previously reported AGM and TLM, the slow ion-acoustic double-layer mode is observed for large pd and intermediate V_d values. The ion-collision effect plays an important role in the formation of double layers. In this regime, low frequency self-oscillation and the period-doubling route to chaos were observed, which is similar to the reported experimental results. The high frequency oscillations in the TLM are caused by a beam–plasma-type instability in the bounded system. A diagnostic parameter, defined as the ratio of the interaction length to the slippage length, is a good measure for period-doubled and chaotic oscillations of this system as shown in other beam–wave interaction systems.

ACKNOWLEDGMENTS

Helpful discussions with Professor M. H. Cho, Professor M. Yoon, and Professor S. H. Kim are greatly acknowledged.

The present studies were supported (in part) by the BSRI-Special Fund of the Pohang University of Science and Technology, the Basic Science Research Institute Program (Ministry of Education 1997, Project No. 97-2439), and the PDP center.

[1] P. Y. Cheung and A. Y. Wong, Phys. Rev. Lett. **59**, 551 (1987).
[2] P. Y. Cheung, S. Donovan, and A. Y. Wong, Phys. Rev. Lett. **61**, 1360 (1988).
[3] J. Qin, L. Wang, D. P. Yuan, P. Gao, and B. Z. Zhang, Phys. Rev. Lett. **63**, 163 (1989).
[4] W. X. Ding, W. Huang, X. D. Wang, and C. X. Yu, Phys. Rev. Lett. **70**, 170 (1993).
[5] C. A. Capeau, G. Bachet, and F. Doveil, Phys. Plasmas **2**, 4650 (1995).
[6] T. Klinger, F. Greiner, A. Rohde, and A. Piel, Phys. Plasmas **2**, 1822 (1995).
[7] W. X. Ding, T. Klinger, and A. Piel, Phys. Lett. A **222**, 409 (1996).
[8] F. Greiner, T. Klinger, H. Klostermann, and A. Piel, Phys. Rev. Lett. **70**, 3071 (1993); F. Greiner, T. Klinger, and A. Piel, Phys. Plasmas **2**, 1810 (1995).
[9] S. Torvén, in *Wave Instabilities in Space Plasmas*, edited by P. J. Palmadesso and K. Papadopoulos (Reidel, Dordecht, 1979), Vol. 74, p. 109.
[10] H. Schamel, Phys. Rep. **140**, 161 (1986).
[11] B. H. Quon and A. Y. Wong, Phys. Rev. Lett. **37**, 1393 (1976).
[12] T. Sato and H. Okuda, Phys. Rev. Lett. **44**, 740 (1981); Ch. Hollenstein, M. Guyot, and E. S. Weibel, *ibid.* **45**, 2110 (1980); C. Chan, M. H. Cho, N. Hershkowitz, and T. Intrator, *ibid.* **52**, 1782 (1984).
[13] C. Chan, M. H. Cho, N. Hershkowitz, and T. Intrator, Phys. Rev. Lett. **57**, 3050 (1986).
[14] M. Bohm and S. Torvén, Phys. Rev. Lett. **66**, 604 (1991).
[15] S. Iizuka, P. Michelsen, J. J. Rasmussen, R. Schrittwieser, R. Hatakeyama, K. Saeki, and N. Sato, Phys. Rev. Lett. **48**, 145 (1982).
[16] D. Alexadroaei and M. Sanduloviciu, Phys. Lett. A **122**, 173 (1987); D. Alexadroaei and M. Sanduloviciu, contributed paper in *the 4th Symposium on Double Layer and Other Nonlinear Potential Structures in Plasmas*, edited by R. W. Schrittwieser (World Scientific, Singapore, 1992), p. 177.
[17] C. K. Birdsall, IEEE Trans. Plasma Sci. **19**, 65 (1991).
[18] T. L. Crystal, P. C. Gray, W. S. Lawson, C. K. Birdsall, and S. Kuhn, Phys. Fluids B **3**, 244 (1991).
[19] T. M. O'Neil, J. H. Winfrey, and J. H. Malmberg, Phys. Fluids **14**, 1204 (1971); T. M. O'Neil and J. H. Winfrey, *ibid.* **15**, 1514 (1972); W. E. Drummond, J. H. Malmberg, T. M. O'Neil, and J. R. Thompson, *ibid.* **13**, 2422 (1970).
[20] J. K. Lee and C. K. Birdsall, Comput. Phys. Commun. **64**, 214 (1991); J. K. Lee and S. J. Hahn, IEEE Trans. Plasma Sci. **19**, 52 (1991).
[21] H. J. Lee, J. K. Lee, M. S. Hur, and Y. Yang, Appl. Phys. Lett. **72**, 1445 (1998); H. J. Lee, J. K. Lee, and M. S. Hur, Bull. Am. Phys. Soc. **42**, 2037 (1997).
[22] M. S. Hur, H. J. Lee, and J. K. Lee, ''A parameterization of nonlinear and chaotic oscillations in beam-plasma diodes,'' to appear in Phys. Rev. E.
[23] S. J. Hahn and J. K. Lee, Phys. Rev. E **48**, 2162 (1993); S. J. Hahn, J. K. Lee, E. H. Park, and T. H. Chung, Nucl. Instrum. Methods Phys. Res. A **341**, 200 (1994); E. H. Park, J. K. Lee, and T. H. Chung, *ibid.* **358**, 448 (1995).
[24] H. J. Lee, J. K. Lee, I. Bae, and M. S. Hur, ''Effects of particle trapping and velocity slippage on the beam-plasma interactions,'' submitted to Phys. Lett. A
[25] I. Langmuir, Phys. Rev. **21**, 419 (1923).
[26] M. Surendra, Plasma Sources Sci. Technol. **4**, 56 (1995); D. Rapp and P. Englander-Goldmen, J. Chem. Phys. **43**, 1464 (1965).